

## **Global Plume-fed Asthenosphere Flow:**

### **(2) Application to the Geochemical Segmentation of Mid-Ocean Ridges**

**Michiko Yamamoto, Jason Phipps Morgan**

*Institute for the Study of the Continents, EAS Department, Cornell University*

*([my83@cornell.edu](mailto:my83@cornell.edu), [jp369@cornell.edu](mailto:jp369@cornell.edu))*

**W. Jason Morgan**

*EPS Department, Harvard University*

#### **ABSTRACT**

Asthenosphere plume-to-ridge flow has often been proposed to explain both the existence of geochemical anomalies at the mid-ocean ridge segments nearest an off-axis hotspot, and the existence of apparent geochemical ‘provinces’ within the global mid-ocean spreading system. We have constructed a thin-spherical-shell finite element model to explore the possible structure of global asthenosphere flow and to determine whether plume-fed asthenosphere flow is compatible with present-day geochemical and geophysical observations. The assumptions behind the physical flow model are described in the companion paper to this study [“Global Plume-fed Asthenosphere Flow: (1) Motivation and Model Development”, Yamamoto et al., this volume.] Despite its oversimplifications (especially the steady-state assumption), Atlantic, Indian, and Pacific MOR isotope geochemistry can be fit well at medium and long wavelengths by the predicted global asthenosphere flow pattern from distinct plume sources. The model suggests the rapidly northward-moving southern margin of Australia, not the Australia-

Antarctic Discordance, is the convergence zone for much plume material in the southern hemisphere. It also suggests a possible link between the strike of asthenosphere flow with respect to a ridge axis and along-axis isotopic peaks.

## INTRODUCTION

It is generally believed that mid-ocean ridges passively sample the shallow mantle beneath the ridge axes. This shallow layer, the asthenosphere, is where the geochemical anomalies found in mid-ocean ridge basalts are also assumed to originate. We think the asthenosphere also plays an important role in mantle flow due to its buoyancy and low viscosity. Asthenospheric flow can transport chemical features from a source hotspot to a mid-ocean ridge, thereby linking geophysical flow to geochemical observations. Along-ridge migration of asthenosphere was first suggested in the papers by *Vogt* [1971], *Vogt and Johnson* [1972; 1975], and *Schilling* [1973] that discussed asthenospheric flow along the Reykjanes Ridge. *Morgan* [1978] proposed the possibility of asthenospheric channels between off-axis hotspots and ridges, and asthenosphere migration in any direction to mid-ocean ridges has also been considered. Now asthenosphere flow is an often-used mechanism to link observed geophysical and geochemical anomalies at mid-ocean ridges to hotspot-ridge connections.

Many sites for hotspot-ridge asthenospheric connection have been proposed. Studies of the Iceland-Reykjanes Ridge connection initiated the concept of plume-fed asthenosphere flow. Now a key Iceland-related question is how far away from Iceland is plume material spreading [*Poreda et al.* 1986; *Fitton et al.*, 1997; *Taylor et al.*, 1997;

*Peate et al.*, 2001]. *Schilling et al.* [1985] and *Hanan et al.* [1986] studied isotopic variation along the southern mid-Atlantic ridge and proposed that isotopic peaks at ridge sites nearest to off-ridge hotspots are observational evidence of flow channels linking these deep mantle plumes to the ridge axis. *Niu et al.* [1999] proposed that lateral asthenospheric flow from Hawaii to the East Pacific Rise (as suggested by *Phipps Morgan et al.* [1995]) left EPR basalts with both enriched and depleted lithologies. Using gravity and topography data, *Small* [1995] proposed hotspot-ridge asthenospheric connections at Louisville, Discovery, Shona and Kerguelen. *Marks and Stock* [1994] suggested the need for along-axis asthenosphere flow from hotspots in order to produce morphologic variation in the Pacific-Antarctic Ridge. *Sempere et al.* [1997] and *Small et al.* [1999] explained variations in geophysical data on the South East Indian Ridge by asthenosphere flow from the Amsterdam-St. Paul hotspot. These previous geophysical and geochemical studies of plume-ridge interaction discussed local hotspot-ridge connections. From these few examples it is difficult to visualize a global pattern of asthenosphere flow.

This study assumes that plume-fed asthenosphere flow is the potential cause of much of the geochemical segmentation observed along the global mid-ocean ridge system. In the companion paper to this study [“Global Plume-fed Asthenosphere Flow: (1) Motivation and Model Development”, Yamamoto et al., this volume.] we have constructed a physical and numerical model for the global flow of buoyant plume-fed material within a thin and laterally heterogeneous asthenosphere layer based on the lubrication theory idealization discussed by *Phipps Morgan et al.* [1995]. In this model asthenosphere is assumed to be brought up by mantle plumes to replenish asthenosphere

consumption (sinks) by plate growth and subduction. Asthenosphere consumption is due to three tectonic activities. The first and largest is plate accretion at mid-ocean ridges, the second is drag-down next to subducting plates at trenches where asthenosphere is entrained by subducting lithosphere, and the third is attachment to the base of the aging and thickening lithosphere. Within this conceptual framework, asthenosphere flow is also shaped by the drag of overriding moving lithosphere; a mechanism explored in earlier models of global asthenosphere trench-to-ridge ‘counterflow’ that are reviewed in the companion paper to this study [“Global Plume-fed Asthenosphere Flow: (1) Motivation and Model Development”, Yamamoto et al., this volume.] Next, we will explore the model’s predicted global asthenosphere flow pattern to test how consistent it is with the spatial patterns of geochemical variations observed at mid-ocean ridges. We find that this conceptually simple model suggests a possible mechanism for the observed boundaries between geochemical provinces of mid-ocean ridge basaltic volcanism.

## **RESULTS**

Figure 1 is a map of the pattern of global asthenosphere flow predicted by this model (See the companion paper [“Global Plume-fed Asthenosphere Flow: (1) Motivation and Model Development”, this volume.] for a detailed description of the assumptions that underlie this prediction). Strong flow occurs beneath the Pacific Basin, because of high plate speeds and the strong ridgeward fluxes from the equatorial Pacific superplume region and Hawaii. In contrast, the Atlantic shows rather weak flows because of its slow spreading rate and the intermediate to weak strengths of its plumes. The Indian Ocean Basin has strong asthenosphere flow in the Central Indian, and reduced flow to north and south.

The predicted flow is quite sensitive to the total plume supply within each basin, as this determines whether or not the basin will push or pull asthenosphere from its neighboring basins. At a smaller scale, the relative plume fluxes between neighboring plumes will affect details of their exact regions of influence along the global spreading system. The companion paper [“Global Plume-fed Asthenosphere Flow: (1) Motivation and Model Development”, this volume.] contains some examples illustrating these sensitivities.

How can this model be tested? A promising geochemical test is that regions of asthenosphere ‘fed’ by each hotspot can be determined, and the boundaries between these regions should be evident at mid-ocean ridges as geochemically distinct ‘provinces’ of mid-ocean ridge basalts. This test is the focus of this paper, and is shown in Figures 2-6. As described in the previous paper, velocities of present-day asthenosphere flow are calculated using present-day plate motions, plate geometries and hotspot strengths — the steady-state assumption. From these asthenosphere velocities, a flow-line is then tracked between each point and its plume source, and an ‘age’ of the asthenosphere at this point is also determined. We used this method to trace flow in all of the asthenosphere; on subsequent figures the resulting plume sources for only those places where asthenosphere is predicted to be supplied by plume upwelling more recently than 100 Ma will be shown as separate hotspot ‘provinces’.

Of course a plate evolution model with varying ocean basin shapes and changing plate motions, plate geometries, and plume strengths should be used for flow-tracking, but this is too-daunting a task for this first cut at global modeling. There has not been a major plate motion reorganization during the most recent ~50 Ma (except perhaps in the

westernmost Pacific). Thus we assume that present-day asthenosphere flow velocities are crudely representative of asthenosphere velocities during the past ~50 Ma in order to make these maps. Where this assumption is obviously bad (e.g. Gulf of Aden or the 'oldest' asthenosphere regions, for example, in the Arctic ocean, western Atlantic, east of Australia and south of Indonesia), the predictions will obviously also be bad. One further simplification was used to generate these figures. The plume strengths we found for continental hotspots (Hoggar, Tibesti, etc.) were all very weak, thus they were all set to zero since they contributed little to the asthenosphere flow within the ocean basins. (See the companion paper in this volume for further discussion of the reasons we currently neglect the effects of subcontinental plume upwelling.) Again, where a continental hotspot could contribute significantly as a source of sub-oceanic asthenosphere (as in the Gulf of Aden), inaccuracies will result.

### **Results: Implications for the structure of global asthenosphere flow**

The flow from Iceland covers the most northern part of the Atlantic (Figure 2). The flow from Iceland going to the south finally meets flow fed from other plumes at 47°N where Iceland's flow is deflected to the west, merging with other flows from the Azores, Madeira and Canary hotspots. The Iceland material also reaches eastward of the Mid-Atlantic Ridge (MAR) to reach England and Scandinavia, but here asthenosphere flow is nearly stagnant. The Iceland material spreads northward to 75°N within 60 Ma. However the influence would reach farther north if given a longer time-interval in which to spread.

The Azores plume feeds a sector-like region to its southwest. Along the ridge, it meets Iceland plume material at 47°N. Azores-fed asthenosphere stretches between 15°N

and 48°N along the MAR (Figure 2b). Eastward of the Azores, the Madeira and Canary plumes ‘block’ eastward flow from the Azores. Madeira and Canary-fed asthenosphere follow similar paths that avoid the center of the Azores plume’s influence and pressure. Their asthenosphere flows both northward to the 47°N region of westward flow and also southwestward to link up with material from the Great Meteor plume. Flow from Canary meets asthenosphere from Cape Verde around ~9°N along the MAR. Cape Verde-sourced asthenosphere fans out from Cape Verde’s latitude of 15°N towards the equator. This flow results in westward-directed flow at the equator, so that North Atlantic asthenosphere does not enter beneath the South Atlantic basin.

Asthenosphere flow beneath the South Atlantic basin is dominated by E-W directed flow except for small radial patterns near hotspots (Figure 3). The flow direction is constantly east to west on the southernmost MAR, due to almost all of the South Atlantic plumes being on the eastern side of the ocean basin. Cameroon, St.Helena, and Fernando da Noronha generate the equatorial flow that blocks North-Atlantic-origin asthenosphere from entering the South Atlantic.

Figure 3 suggests that a plume province boundary also exists in the South Atlantic near 25°S. Asthenosphere north of the boundary is supplied with material mixed from Cameroon, Fernando, Ascension, St Helena and Martin Vaz; regions south of the boundary are supplied by Vema, Tristan, Gough, Discovery and Bouvet. In the north, St Helena appears to be the main asthenosphere source for the ridge, while Cameroon’s flow area tapers off toward the ridge to become too narrow at the ridge to be a major source. Other plumes in the north province are located in west of the ridge and their material flows to the west — thus they do not influence the ridge’s geochemistry. South of the

25°S boundary, source hotspots are located to the east of the ridge and all of them except Vema supply material that flows westward to cross the ridge. Tristan and Gough have similar patterns. Their main stream fans westward to supply the ridge between 25° and 50°S. One side branch flows eastward to the western coast of Africa, one to the Antarctic, and a third flows south of Africa to the Indian ocean. Flow from Discovery has three similar branches. Bouvet-fed asthenosphere mainly flows to the Antarctic but a smaller branch goes into the Indian Ocean basin, too. The plume material of Tristan, Gough, Discovery and Bouvet together flows into the Indian ocean where it is pulled eastward by the pressure gradient in the southern Indian ocean, through the Rodrigues Triple Junction and finally converging to the south of Australia.

The flow tracking shows that the Rodrigues Triple Junction may be a distant ‘floodgate’ for many hotspots (Figure 4). Asthenosphere fed from the Tristan-group hotspots (Tristan, Gough, Bouvet and Discovery in Atlantic) and also Crozet, Marion, Ob-Lena and Reunion in Indian ocean all pass beneath the region of this Triple Junction. The Tristan-group’s flow track divides Indian Ocean into two provinces. The northern province is mainly filled with material from Reunion and Comores (and Afar) plumes. This flow tracking suggests that Reunion material alone supplies the Central Indian Ridge, while the Comores (and Afar) plumes are the source region for the Carlsberg Ridge and Gulf of Aden. Flow from Reunion does not overlap with flow from these others.

In the south Indian Ocean province, five hotspots, Ob-Lena, Marion, Crozet, Kerguelen and Heard are located close in latitude around 50°S and grouped into two longitudinal regions of 30°E for Ob-Lena, Maria, and Crozet, and 60°E for Kerguelen and

Heard. All asthenosphere fed from these hotspots heads eastward (pushed by the excess of South-Atlantic plume supply of asthenosphere) to finally converge to the south of Australia at 110°E (Figure 5a). Kerguelen and Heard, closer to this convergence point, feed flow that goes straight through the Southeast Indian Ridge (SEIR). In contrast, Marion, Crozet and Ob-Lena feed winding and splitting flow that avoids the region fed by Kerguelen and Heard (Figures 4 and 5). Their branches have two contact points with the SEIR, one west of 80°E, one east of 98°E (Figure 5b). The direction of asthenosphere flow beneath the SEIR is consistently perpendicular to the ridge, while along-ridge flow dominates beneath the Southwest Indian Ridge.

In the Pacific Basin, Hawaiian plume material feeds a large area beneath the northern Pacific, while other plumes produce bands of material that fill up the rest of the northern area (Figure 6a). The hotspots along the western coast of the North American continent, Bowie, Cobb and Guadalupe, produce strong and narrow southeastward along-coast flow to the East Pacific Rise (EPR). Bowie and Cobb's flow tracks overlap, and both cross the EPR at 15°N. Flow from Guadalupe goes along the ridge with material from the Galapagos plume until it meets Bowie and Cobb's across-ridge flow. The plumes beneath the "Super Swell" region [McNutt and Fischer, 1987], Marquesas, Society, Pitcarn, Line and Macdonald recharge most of the southern part of the Pacific basin. Foundation and Louisville plume material flows southwestward along the edge of flow from the Super Swell.

Plume material originating beneath the Pacific plate appears to have two main destinations. One is toward the western Pacific trenches. This is the main destination for material from the Hawaiian, Caroline, Samoa, Marquesas and Society hotspots. The other

destination is the southern continental margin of Australia, which is also the destination for asthenosphere from plume in the south Indian basin. This rapidly moving continental margin is an asthenospheric ‘sink’ that pulls asthenosphere fed from plumes beneath the Pacific plate and from the Scott and Balleny plumes beneath the Antarctic plate in addition to several Indian plumes. Other Pacific-basin hotspots beneath the Nazca plate, namely Galapagos, San Felix and Juan Fernandez, feed flow that does not terminate south of Australia. Instead, they flow to south, then turn westward after passing beneath the Chile Rise, just reach the southern part of EPR, then turn southwards once more (Figure 6a). The direction of flow beneath the EPR and Pacific-Antarctic Ridge changes with latitude, there is ridge-parallel flow north of 15°S, across-ridge flow between 15°S and the southern end of the EPR, and ridge-parallel flow beneath most of the Pacific-Antarctic Ridge.

An intriguing respect of this predicted asthenosphere flow pattern is the ‘vortex’ beneath the EPR near 30°S — the fastest spreading region in the world where two micro plates currently exist. This area influences flow from many plumes beneath the Pacific plate (Figure 6b), namely Hawaii, Bowie, Cobb, Marquesas, Pitcairn, Easter and Foundation. All are located north of or close to this region. The flow vortex is a very persistent feature in our model, occurring even when the relative balance between Pacific plume strengths is changed or even with other plume sources within the Pacific. We think it is due to the large ridge consumption of asthenosphere in this region and the large ‘pull’ of material beneath the Indian and Pacific basins to the great sink south of Australia.

## DISCUSSION

The calculated asthenosphere flow pattern can be compared to geochemical 'province' boundaries along the mid-ocean ridge system and to maps of seismic wavespeeds and anisotropy in the shallow upper mantle. These comparisons show promising agreement between the calculated flow pattern and these geochemical and seismic observations. For example, maps of seismic azimuthal anisotropy suggest a S-N flow direction in the area between Australia and Antarctica, and potential W-E flow between Hawaii and the EPR [*Montagner and Tanimoto, 1990; Leveque et al., 1998; Montagner and Guillot, 2002; Gaboret et al., 2003*], both consistent with our results. In the Atlantic, *Ritsema and Allen [2003]* suggest the asthenosphere beneath the MAR at 14°N lies in the fastest velocity zone along the MAR, while our flow model suggests that the 14°N is the farthest point from the source hotspot. In other words, both are consistent with the possibility that 14°N is the 'coldest' region along the MAR.

While comparisons between seismic wavespeed maps and flow may indicate the most extreme asthenosphere province boundaries such as the AAD, in general seismic velocities are slow beneath the spreading center system, and thus cannot be easily used to locate more subtle asthenosphere province boundaries. However, geochemical isotopic province boundaries along the reasonably well sampled mid-ocean ridge system (typically at least one sample per 100 km length along-ridge) do exhibit finer small-scale variability that is interesting to compare to the province structure predicted by the flow model.

Next we discuss specific regional aspects of the flow pattern, comparing isotopic/chemical patterns along the mid-ocean ridge to model inferences under the

assumption that the connections between hotspots and mid-ocean ridges in Figures 8-12 have existed long enough so that the ridge material has had time to flow from its source plume. In general this assumption seems plausible because most plume sources are calculated to reach the ridge they cross within 30 Ma, and during this time interval plate motions have remained relatively stable.

### **Atlantic ocean basin**

Our results imply that Atlantic athenosphere has four distinct domains separated by three internal boundaries. All our predicted asthenosphere province boundaries are EW-oriented. They cross the MAR at 48°N, 4°S, and 25°S respectively. *Dosso et al.* [1993] compiled  $^{87}\text{Sr}/^{86}\text{Sr}$ , La/Sm and Nb/Zr data along the northern MAR between 10° and 74°N (Figure 7). Along-ridge variations in these trace element ratios show four peaks at 64°N, 45°N, 39°N and 14°N. Because these four positive peaks appear at the latitude of Iceland, Azores and Cape Verde, their hotspot-ridge connections were suggested by *Phipps Morgan et al.* [1995].

Our model supports the idea that the peak at 64°N results from the injection of the Iceland material and the peaks at 45°N and 39°N are from the Azores. However, the model does not support the proposed relationship between the peak at 14°N and the Cape Verde hotspot. Instead it suggests that the changes at 14°N may be related to the injection of Canary, Madeira, or Great Meteor plume material within a narrow region at this latitude. Several geochemical observations do not favor a possible link between the Cape Verde plume and the 14°N section of the MAR. For example, the material at 14°N differs from the Cape Verde hotspot basalts in its  $^4\text{He}/^3\text{He}$  signature. The  $^4\text{He}/^3\text{He}$  ratio

suddenly rises at 14°N [*Staudacher et al.*, 1989; *Bonatti et al.*, 1992], while low  $^4\text{He}/^3\text{He}$  in Cape Verde has been reported [*Christensen et al.*, 2001; *Doucelance et al.*, 2003] (however, this evidence is not conclusive, see later discussion regarding St. Paul and Kerguelen). Furthermore, *Schilling et al.* [1994] studied Pb-Nd-Sr systematics along the ridge and found that the 14°N anomaly is more similar to the 1.7°N anomaly and distinct from the signature of hotspots in northern Atlantic. They attributed the 1.7°N anomaly to the Sierra Leone hotspot at 5°N, 10 degrees south of Cape Verde. However, if the 14°N anomaly is also due to flow of material from the Sierra Leone plume, it would need the reverse sense of flow than that predicted from our model. The plume source list for our flow calculation does not include a possible Sierra Leone plume, but the southward flux north of the equator is quite strong so that adding a Sierra Leone plume is not likely to change the pattern. We think it more likely that either Canary or Madeira plume material may be ‘nosing’ into the MAR here, or that this represents the northern limit of the Cape Verde plume’s influence on the ridge axis — but then leaving a question as to why its influence should be more pronounced here than to the south.

Westward asthenosphere flow dominates the south Atlantic — the effects of hotspots east of the ridge are predicted to be seen at roughly the same ridge latitude as that of the source hotspots. Observed anomalies in  $^4\text{He}/^3\text{He}$ , La/Sm and Nb/Zr are evident at the latitudes corresponding to Ascension, St. Helena, Tristan and Gough, however the  $^{206}\text{Pb}/^{204}\text{Pb}$  peak is not seen in the Tristan and Gough area (Figure 8), possibly because they have an originally low ratio [*Dickin*, 1995]. All data, except He, show no signal between 20°S and 30°S, a region with no nearby hotspots [*Schilling et al.*, 1985; *Hanan et al.*, 1986; *Graham et al.*, 1992]. Discovery plume material injected at 43°S is predicted

to flow southward to reach the ridge south of 47°S, in agreement with *Douglass et al.* [1999]'s observations. A flow boundary in the South Atlantic runs perpendicular to the ridge at 25°S where the St Helena flux meets against Tristan and Gough flux. In this region the asthenosphere flux becomes more stagnant. This area was studied by *Graham et al.* [1996] who focused on He anomalies. They discovered a He signal at 26°S and speculated that more than two mantle components may mix or meet in that region.

### **Indian ocean basin**

Our model suggests two asthenosphere domains in the Indian Ocean. The boundary separating the Indian Ocean into northern and southern parts goes through the Rodriguez Triple Junction (RTJ). The RTJ region receives flow from the Discovery, Tristan and Gough (Tristan-group) plumes in the South Atlantic, although the long distance and long predicted asthenospheric travel-time between these plumes and this section of the ridge make this inference more speculative to us than other inferences in this paper. However, we cannot dismiss this possibility because the Triple Junction has existed since the upper Cretaceous, which is significantly longer than the time for material to travel from the Tristan-group and the Triple Junction, and furthermore, because this inference is consistent with geochemical evidence. The Triple Junction is reported to be a peculiar region in isotopic composition, basalts from here have relatively high  $^{87}\text{Sr}/^{86}\text{Sr}$  and low  $^{206}\text{Pb}/^{204}\text{Pb}$ , and these ratios differ strongly from the isotopic chemistry of adjacent ridges [*Price et al.*, 1986; *Mahoney et al.*, 1989; 1992]. *Michard et al.* [1986] suggested that the Rodriguez Triple Junction basalt source was produced by

mixing with a mantle of extremely low  $^{206}\text{Pb}/^{204}\text{Pb}$  and low  $^{143}\text{Nd}/^{144}\text{Nd}$  but intermediate to high  $^{207}\text{Pb}/^{206}\text{Pb}$  and  $^{87}\text{Sr}/^{86}\text{Sr}$ . This characterization is like that of Tristan-group basalts [Graham *et al.*, 1992; Dickin, 1995]. Even if doubts remain about the connection between the South Atlantic and Rodriguez Triple Junction, our result and isotopic studies agree that the Rodriguez Triple Junction lies at the geophysical and geochemical boundary between distinct Indian asthenosphere provinces.

The connection between South Atlantic and Indian Ocean seems to be associated with the Sr-Pb “Dupal anomaly” [Hart 1984; Dupre and Allegre, 1983]. The Dupal anomaly shows an isotopic similarity between the Tristan-group, Kerguelen, and Ninetyeast ridge. Grouping Ninetyeast with Kerguelen-plume volcanism is acceptable because the old and dead Ninetyeast ridge was formed prior to ~46Ma when the Ninetyeast Ridge was near the plume and mid-ocean ridge [Royer and Sandwell, 1989]. Therefore it is natural that Ninetyeast Ridge chemistry shows Kerguelen’s signature, but the signature is from old rather than recent ridgeward flow.

The three mid-ocean ridges within the Indian Ocean basin, the Central Indian Ridge (CIR), Southwest Indian Ridge (SWIR), and Southeast Indian Ridge (SEIR) each have their own characteristic geometric and geochemical relationship with their source hotspots. The CIR shows a simple signature reflecting a single Reunion plume source. It has  $^{87}\text{Sr}/^{86}\text{Sr}$ ,  $^{206}\text{Pb}/^{204}\text{Pb}$  and  $^{143}\text{Nd}/^{144}\text{Nd}$  signals similar to those of Reunion basalts that appear on the ridge at the same latitude as the hotspot [Mahoney *et al.*, 1989]. This phenomenon requires eastward flow from the Reunion, which is a feature of our model.

The northern limit of the Reunion flow on the ridge is located at about 8°S which corresponds to the axial fissuring area that is the morphological transition zone

between the CIR to the Carlsberg ridge, although *Mahoney et al.* [1989] positioned the limit onto the Marie Celeste FZ at 16°S, and assigned the 70 km south of the Marie Celeste FZ to Reunion's influence based on the detectable Reunion-like isotope signal. This 70 km-long ridge section is the closest to the hotspot in the sampling points along the ridge, therefore it is reasonable the area shows such a strong peak or the area could well have a strong asthenosphere flow channel connecting it to the Reunion hotspot [*Morgan, 1978*].

The SWIR has three nearby hotspots, one is the Marion hotspot only 180 km away from the ridge axis, one is the Ob-Lena located very close to the Marion, and the other is the Crozet at about 500 km away from the ridge. SWIR isotope data do not provide direct images of the connection between the near-ridge hotspots and the isotopic signals in spite of their proximity. There are big spikes around 40°E in Sr, Pb and Nd [*Mahoney et al., 1992*], and these isotopic compositions are not like those of either Marion or Crozet. (*Mahony et al.* [1992] considered these signals to arise from old Madagascan lithosphere stranded in that area.) Actually small peaks in Sr and Nd resembling Marion's composition do exist, but not at the closest point on the ridge to the Marion, instead about 550 km east of it. Other places along the ridge show no chemical traces similar to nearby hotspots.

The asthenosphere flow model suggests a possible correlation between local asthenosphere flow directions and the existence (or absence) of hotspot signal in this SWIR area. The place having Marion's signal is the only place having across-ridge flow from the Marion source hotspot. All other sites along the SWIR are regions with a strong along-ridge flow, where plume material from Marion, Ob-Lena and Crozet flow together

along-axis. This perhaps mixes the material and subdues the geochemical variation along the ridge.

Interaction between Kerguelen-Heard hotspots and SEIR has been proposed by many earlier studies [*Dosso et al.*, 1988; *Small*, 1995; *Johnson et al.*, 2000; *Weis and Frey*, 2002; *Mahoney et al.*, 2002], and our model also indicates that Kerguelen-Heard material flows to the SEIR and extends over rather large area. Asthenosphere flow at the SEIR is consistently ridge-perpendicular in our model (Figure 5). The isotope variability here (Figure 9) is bigger than along the SWIR but less than seen at the southern MAR near St Helena (Figure 8), another region of persistent across-axis asthenosphere flow. We think its smaller amplitude in comparison to that on the MAR may reflect the greater distances between the ridge and its source hotspots. Even the closest, Kerguelen, is 1400 km away from the ridge and Marion, the most remote source here, is 6600 km away.

Although across-ridge flow is predicted by our model, many previous studies suggested the existence of eastward along-ridge flow from inferences based on the variations in ridge depth, morphology and segment geometry east of Amsterdam–St. Paul [*Sempere et al.*, 1997; *Graham et al.*, 1999; *Small et al.*, 1999]. In detail, they suggested Amsterdam–St. Paul is the source plume for along-ridge flow resulting in a mantle temperature gradient from ‘hot’ west of Amsterdam–St. Paul to ‘cold’ at the Australian-Antarctic Discordance (AAD). (In contrast to these authors, we think Amsterdam – St. Paul is not a separate plume but a manifestation of plume-to-ridge flow from the Kerguelen Plume.) This change in sub-ridge temperature structure was considered to be the cause of the transformation from an axial high with shallow depth and longer segmentation along the western SEIR to a median valley with short segmentation at the

AAD [*Ying and Cochran, 1996; Sempere et al., 1997*]. Spreading rate variations cannot be the cause, since the spreading rate remains constant along this ridge. However, along-ridge flow is not a unique way to explain this variation in thermal structure. With the same logic that the distance from a plume source to the ridge will shape the temperature of the asthenosphere feeding a given section of the ridge, our model also suggests a similar gradient from hotter west to colder east. Furthermore, the dynamic topography calculated from pressure distribution (Figure 1) deepens to east along the ridge in agreement with observed axial depth variations.

Some previous studies appear to be conflict with the along-ridge flow hypothesis. *Mahoney et al. [2002]* studied isotopic variations along the SEIR and found that the regional isotope pattern cannot be explained by the eastward flow. If eastward flow exists then variations in isotopic ratios should show a monotonic change to east, but actually the variations show several peaks along the ridge (Figure 9). *Ying and Cochran [1996]* studied the detailed morphology of the SEIR and revealed the ridge continues to become shallower away from the Amsterdam–St. Paul to the east and that an axial valley is present just east of the Amsterdam–St. Paul. Therefore they concluded that the Amsterdam–St. Paul plume was not the source of along-ridge flow to east. They also located the axial-high between 82°E to 104°E. This region is exactly where Kerguelen influences the ridge in our model. Kerguelen is the strongest and the nearest hotspot to the SEIR, therefore the thermal effects causing the axial-high morphology are most plausibly related to Kerguelen.

Our across-ridge flow hypothesis has at least one weakness. Across-ridge flow does not intuitively explain the V shapes on the seafloor along the ridge, which has been

proposed to be traces of eastward mantle propagation [*Sempere et al.*, 1997]. However those V shapes have migrated for small distances along-axis (~150 km) compared with V-shaped features on Pacific-Antarctic Ridge or Northern MAR (>1000 km). Perhaps these small V shapes are not the surface expression of asthenosphere flow but instead a more superficial phenomenon due to persistent eastward ridge-propagation away from the central shallow region.

### **Pacific ocean basin**

The East Pacific Rise (EPR) geochemistry is characterized by much less variability compared to other ridges. Only rather broad and low peaks in  $^{206}\text{Pb}/^{204}\text{Pb}$  and  $^{87}\text{Sr}/^{86}\text{Sr}$  between 15°S and 21°S are resolvable. [*Macdougall and Lugmair*, 1986; *Bach et al.*, 1994; *Niu et al.*, 1999; *Lehnert et al.*, 2000, (PETDB)] This isotopic variation has not been explained as being due to plume-ridge connections because of the absence of the nearby hotspots, and cannot be explained by relationships with second-order segmentation because there are no such systematic relationships. *Bach et al.* [1994] suggested these Pb and Sr peaks relate to either an incipient mantle plume near 17°S or large-scale mantle heterogeneity. *Mahoney et al.* [1994] interpreted these peaks together with a He narrow peak at 17°S as an expression of a mantle flow with a discrete heterogeneity as entering into the ridge system at 15.8°S and then migrating to 20.7°S. On the other hand, our model suggests the 15-20°S peak is associated with a region of across-ridge flow. Model flow directions change along the ridge, with along-ridge flow north of 15°S, and across-ridge between 15°S-25°S. This is consistent with the relationship between flow direction and

isotopic peaks seen in the Indian Ocean basin, although opposite to *Mahoney et al.* [1994]'s inference of along-ridge flow southward of 15°S.

*Vlastelic et al.* [1999]'s results match well with our predicted flow models. They compiled Nd, Sr and Pb data along the EPR and Pacific-Antarctic Ridge (PAR), and created a  $\delta\text{Nd-Sr}$  and  $\delta\text{Sr-Pb}$  diagnostic to discriminate between ridge source provinces (Figure 10). According to this discriminant, the ridge can be divided into four distinct geochemical regions with a data gap between the Juan Fernandez microplate and the Vacquier FZ. The four divisions are, starting from the north: (1) the area from 15°N to north of Easter ( $\delta(\text{Nd-Sr}) > 0$ ,  $\delta(\text{Sr-Pb}) > 0$ ); (2) the area from south of Easter to the southern boundary of the Juan Fernandez microplate ( $\delta(\text{Nd-Sr}) < 0$ ,  $\delta(\text{Sr-Pb}) < 0$ ); (3) the area from south of Eltanin FZ to Udintsev FZ ( $\delta(\text{Nd-Sr}) > 0$ ,  $\delta(\text{Sr-Pb}) > 0$ ); and (4) the ridge south of Udintsev FZ ( $\delta(\text{Nd-Sr}) < 0$ ,  $\delta(\text{Sr-Pb}) < 0$ ). In other words, the ridge south of Easter generally has the isotopic signature of ( $\delta(\text{Nd-Sr}) < 0$ ,  $\delta(\text{Sr-Pb}) < 0$ ) but only around the Eltanin FZ do ridge basalts show  $\delta(\text{Nd-Sr}) > 0$ ,  $\delta(\text{Sr-Pb}) > 0$ . *Castillo et al.* [1998] also reported a possible change in the ridge's mantle source at the Heezen Transform of the Eltanin FZ system.

The other two ridges connecting to the EPR, the Galapagos Rise and the Chile Rise, were sorted by *Vlastelic* into the group with ( $\delta(\text{Nd-Sr}) > 0$ ,  $\delta(\text{Sr-Pb}) > 0$ ). These isotopic characteristics are also explicable in terms of our flow model if asthenosphere from South Pacific plume sources has  $\delta(\text{Nd-Sr}) > 0$ ,  $\delta(\text{Sr-Pb}) > 0$  while asthenosphere from North Pacific or Nazca plumes has ( $\delta(\text{Nd-Sr}) < 0$ ,  $\delta(\text{Sr-Pb}) < 0$ ). This is a possible explanation for why the regions around the Eltanin FZ and the southern Chile Rise have

the same geochemical signature — because both regions are predicted to have the same Juan Fernandez plume source material.

Geophysical implications of an asthenosphere flow ‘vortex’ underlying the EPR between 25-35°S (Figure 6a) are discussed in the companion study in this volume. The region above this vortex is characterized by the fastest present-day spreading rates (160 mm/yr). A large flux of asthenosphere is being pulled into this area to replenish the asthenosphere-consuming creation of compositional lithosphere at the world's fastest spreading mid-ocean ridge. The Easter hotspot is the nearest of the involved hotspots to this area. However Easter plume signals are not observed, instead, high  $^{87}\text{Sr}/^{86}\text{Sr}$  was reported on the ridge at about the latitude of the Easter hotspot, although the Easter itself has  $^{87}\text{Sr}/^{86}\text{Sr}$  presumed to be too low to be the source of that anomaly [Macdougall and Lugmair, 1986]. This isotopic signal could result from contamination with asthenosphere from the “SOPITA” (South Pacific Isotopic and Thermal Anomaly) [Staudigel *et al.*, 1991] region to the west that is recognized as one of the highest  $^{87}\text{Sr}/^{86}\text{Sr}$  plume sources in the world. This agrees with the predicted asthenosphere flowpaths which show both Marquesas and Pitcairn plume materials being mixed into this area.

### **Australian-Antarctic Discordance (AAD)**

Many previous studies have suggested along-ridge asthenospheric flow towards the Australian-Antarctic Discordance (AAD) and downwelling beneath the AAD in a “cold-spot”. The AAD’s rough topography, closely spaced transform faults, regional gravity low and low magnetic amplitudes are considered to reflect regionally cooler

mantle temperature and lower than normal melt production beneath it, which led many scientists to the concept of mantle downwelling beneath this region. The west-pointing and east-pointing V-shapes in both sides of AAD have also been cited as evidence of flow converging towards the AAD. Geochemically, a sharp compositional boundary between Pacific and Indian MORB is also found beneath the eastern AAD.

Although these many observations seem to be consistent with asthenosphere flow into the AAD, our model suggests a slight variation to this scenario — perhaps asthenosphere flow is converging to the south of the rapidly moving Australian continental lithosphere, not along the ridge to the AAD ridge segments themselves (Figures 5a and 6a). In our model, the “suction” forcing this asthenosphere flow is due to the very fast northward motion of Australia — the large lithosphere thickness change between the craton and oceanic lithosphere at Australia’s southern continental margin creates a northward moving ‘void’ that must be replenished by northward flow of asthenosphere. Currently this is the location where thick continental cratonic lithosphere is moving most rapidly away from an ocean basin. The geophysical argument for along-ridge flow convergence beneath the AAD is that the AAD contains the maximum or minimum value in topography, gravity, and seismic anomalies along the Pacific-Indian ridge system. However, if the entire basin between Australia and Antarctica is considered as a whole, then the maximum or minimum geophysical anomalies lie south of Australia (i.e. north of the mid-ocean ridge) rather than at the ridge axis segments of the AAD. For example, residual topography and gravity anomalies south of Australia are lower than these anomalies within the AAD [Veevers, 1982; Kido and Seno, 1994; Gurnis *et al.*, 2000]. Furthermore, *Christie et al.* [1998]’s results indicate that lateral

mantle migration to the AAD is constrained to a narrow, relatively shallow region, directly beneath the easternmost segment of the spreading axis. Deeper south-to-north asthenosphere flow beneath the region does not conflict with these observations, and yet still predicts the existence of a strong geochemical boundary along the ridge segments within the AAD.

### **Flow direction and He isotopic anomalies**

Comparing the predicted flow directions and MORB isotopic anomalies along the ridge axis shows the following potential empirical relationships between them.

1) Across-ridge flow projects the asthenosphere source plume compositions onto the ridge axis.

2) Across-ridge flow generates He-isotope peaks at the leading edge of each plume province, with the amplitude of the peak apparently unrelated to the distance between the source plume and ridge axis.

3) Along-ridge asthenosphere flow results in little to no variability in MORB isotopic signals.

4) 1, 2 and 3 above do not occur when the hotspot is located just beneath or close to the ridge. In this case, there is strong evidence for along-ridge flow with the isotopic peaks reflecting the plume's mantle source composition.

Along-ridge asthenosphere flow is prominent at the SWIR, PAR, and the northern parts of the EPR. All of these regions show very flat patterns in their Pb-Sr-Nd isotope ratios [Mahoney *et al.* 1992; Lehnert *et al.*, 2000, (PETDB) ; Vastelic *et al.*, 2000]. This

correlation occurs even when the hotspots are located rather near the ridge (e.g. SWIR and northern EPR), while the across-ridge asthenosphere flow produces isotopic peaks on the ridge even after there has been long-distance travel from the source hotspots to the ridge (e.g. CIR, southern MAR and SEIR). *Vastelic et al.* [2000] shows a good example. They noted that the Udintsev FZ is a boundary between a pattern of isotopic variability north of the FZ to little isotopic variability south of the FZ. Our model predicts that the Udintsev FZ is a boundary between across-ridge asthenosphere flow direction to its north and along-ridge flow to its south. Perhaps the asthenosphere flow direction at a ridge (across-axis vs. along-axis) may be a key factor underlying these observed MORB isotope systematics. Along-ridge flow may better mix material from multiple plume sources, thus subduing the distinct influence of individual plumes.

It is well known that He isotopes exhibit peculiar behavior that is decoupled from those of another isotopes (e.g. [*Rubin and Mahoney, 1993*]). The reasons for this are not yet explained in terms of any global empirical rules. We suggest that the He signal may be strongly related to across-ridge asthenosphere flow. For example, along the southern MAR, He peaks appear not only at hotspot-related areas but also at no-hotspot areas, although Pb, Nb/Zr, and La/Sm peaks appear at only the latitude of the hotspots and have no peaks at non-hotspot areas (Figure 8) [*Graham et al., 1992*]. The EPR (Figure 11) has a narrow He peak at 17°S [*Mahoney et al., 1994*] which is the only place having across-ridge flow along the EPR. The SEIR shows periodic peaks in He variation along the ridge (Figure 9) (from [*Graham et al., 2001*]). Figures 9 and 11 indicate that the locations with these He peaks seem to be well correlated with province boundaries between different plume sources. On the other hand, when the plume lies directly beneath the spreading

center (e.g., Iceland), then the He-peak is much broader and slowly decays away with increasing distance from the plume.

The good agreement between the locations of He peaks along the SEIR with the predicted boundaries between regions of plume influence on SEIR (Figure 9) suggests that there is a common mechanism causing these He peaks. From the east, one He peak would be linked to flow from Gaussberg, one the Crozet-group, one Heard, and the central one to Kerguelen instead of the proposed Amsterdam-St. Paul hotspot located near the western edge of the Kerguelen plume influence. (In the simplest interpretation consistent with these results, Amsterdam-St. Paul hotspot volcanism would not be fed from a deep underlying plume of mantle upwelling, but instead would lie at the distal end of a region of lateral plume-to-ridge asthenosphere flow between Kerguelen and the SEIR (see Yale and Phipps Morgan (1998)). This scenario has the conceptual strength that it makes the influence of Kerguelen on the ridge like that of its neighboring plumes, just with a larger influence along the ridge because of Kerguelen's larger plume flux.) Therefore, as the flow model suggests their physical connection, this high  $^3\text{He}$  content would originate in Kerguelen plume, not in a separate Amsterdam-St. Paul plume.

Kerguelen's He has been observed to have a lower  $^3\text{He}/^4\text{He}$  ratio than MORB. Some studies have suggested that Kerguelen's basaltic volcanism is contaminated by old materials in the thick lithosphere just before eruption, thus they estimate the He ratio in the Kerguelen source composition to be higher than the observed ratio [Barling *et al.*, 1994; Hilton *et al.*, 1995; Nicolaysen *et al.*, 2000; Coffin *et al.*, 2002; Frey *et al.*, 2002; Mahoney *et al.*, 2002]. However, no study has mentioned the effect of the thick lithosphere overlaying Kerguelen hotspot on the He content in lateral plume-to-ridge

flow from the Kerguelen plume. We suggest that the limited melting at Kerguelen keeps much of the He from the Kerguelen plume source in the (plume-fed) asthenosphere, to be more completely extracted when it ascends again to melt beneath the SEIR.

Recent seismic tomography and geochemical studies have discussed whether  $^3\text{He}/^4\text{He}$  truly is a fingerprint of major (or deep-rooted) plumes [Foulger and Pearson, 2001; Meibom *et al.*, 2003]. We are highly influenced by the fact that the Iceland plume influences Sr, Pr, and He isotopes along the Reykjanes Ridge [e.g. Breddam *et al.*, 2000; Hilton *et al.*, 2000], and that the Iceland plume source can be richer in He when it first upwells and melts than other asthenosphere that melts beneath a spreading center. We favor the interpretation that high  $^3\text{He}/^4\text{He}$ , when seen, is a diagnostic of the dominance of a He-contribution due to melt-extraction from a component of more ‘primitive’ mantle that makes up a fraction of the upwelling mantle plum-pudding, but that plumes also contain low  $^3\text{He}/^4\text{He}$  components (e.g. enriched radiogenic plum components) so that the absence of high  $^3\text{He}/^4\text{He}$  hotspot basalts does not imply the necessary absence of a deep plume. This interpretation is discussed in more detail by Phipps Morgan and Morgan (1999).

### **Transport distance and the ‘survival’ of a plume’s isotope signal**

The Crozet-group has two output sites along the SEIR. One is north of Amsterdam-St. Paul, the other far to the east around 116°E. The predicted eastern output region has a gentle Pb peak at the middle of the flow range [Mahoney *et al.*, 2002], while

the northern contact region shows no visible peaks [Mahoney *et al.*, 1989; Lehnert *et al.*, (PETDB)], although both routes involve about the same distance of lateral asthenosphere flow. A possible difference between them may be caused by the difference in lithospheric thickness along their route to the output point. The route to the northern output point is consistently capped with relatively young and thin lithosphere. On the other hand, the asthenosphere flowpath to the eastern output region underlies old thick lithosphere whose thickness is constant or increasing until about 1000 km before the ridge. Niu *et al.* [1999] explained how an enriched component could possibly survive over the long distance between Hawaii and EPR.

If thick lithosphere suppresses decompression melting during the course of lateral asthenospheric transport, then the plume lithology can be preserved in spite of a long horizontal travel path — as long as it is progressive melt extraction, and melt-extraction alone that removes the distinctive plume-component signals from the plume-fed asthenosphere that forms the MORB source [Phipps Morgan, 1997; 1999; Phipps Morgan and Morgan, 1999]. If this conceptual framework is true, then the Crozet group would be in a similar or even more ‘advantageous’ situation than long-distance transport from Hawaii to the EPR because the predicted flow from the Crozet group consistently occurs beneath thick old lithosphere, while lithosphere along the route from Hawaii gradually thins towards the EPR. Therefore, we think it feasible that the Pb peak at 116°E could originate from the Crozet group.

### **Summary and assessment of this exercise in geochemical pattern matching**

This initial comparison between our predicted flow-field for sub-oceanic asthenosphere and observed geochemical province boundaries along the global spreading system has yielded intriguing but not definitive results. In the Atlantic Ocean basin a one-to-one match is often possible — but in this basin several poorly determined parameters in the flow model have been tuned to match the regional geochemical province boundaries. Nevertheless it is encouraging that a match was possible. In the other ocean basins no such tuning was necessary since relative hotspot upwelling fluxes beneath moving plates could be crudely constrained by rates of the past 5-10 Ma of magma production at their associated hotspots. (See *White*[1994] and *Phipps Morgan* [1997] for two similar estimates that were obtained using somewhat different geophysical approaches). In these basins the model asthenosphere flow predictions raise several intriguing possibilities to explain observed geochemical variations along the spreading center. They suggest that the AAD is not a region of along-ridge downwelling, but rather simply a region of convergence between Indian and Pacific plume material that is being ‘driven’ by the rapid northward migration of the Australian craton. It suggests that cross-ridge asthenosphere flow and along-ridge flow may be associated with different geochemical fingerprints. It also suggests that individual plumes, as their upwelled plume material flows across a ridge axis, may generate He anomalies along the leading edge of each flow domain. We remain hopeful that the asthenosphere flow modelling technique developed in this work and the companion study will be a useful tool to further test whether the paradigm of a plume-fed asthenosphere will ultimately provide a better conceptual framework with which to understand the flow and melting of Earth’s upper mantle.

*Acknowledgements.* We would like to acknowledge Morgan A.L. Crooks, Jörg Hasenclever, Walter Smith, and Mara Yale for their help during the 12 years of gestation of this work. We also thank Don Anderson, Gill Foulger, Donna Jurdy, and Lars Rüpke for helpful reviews.

## REFERENCES CITED

- Bach, W., Hegner, E., Erzinger, J., and Satir, M., 1994, Chemical and isotopic variations along the superfast spreading East Pacific Rise from 6° to 30°S: *Contrib. Mineral. Petrol.*, v. 116, p. 365-380.
- Barling, J., Goldstein, S., L., and Nicholls, I.A., 1994, Geochemistry of Heard island (southern Indian Ocean): Characterization of an enriched mantle component and Implications for enrichment of the sub-Indian Ocean mantle: *J. Petrology*, v. 35, p. 1017-1053.
- Bonatti, E., Peyve, A., Kepezhinskas, P., Kurentsova, N., Seyler, M., Skolotnev, S., and Udintsev, G., 1992, Upper mantle heterogeneity below the Mid-Atlantic Ridge, 0-15N: *J. Geophys. Res.*, v. 97, p. 4461-4476.
- Breddam, K., Kurz, M.D., and Storey, M., 2000, Mapping out the conduit of the Iceland mantle plume with helium isotopes: *Earth Planet. Sci. Lett.*, v. 176, p. 45-55.
- Castillo, P.R., Natland, J.H., Yaoling, N., and Lonsdale, P.F., 1998, Sr, Nd, and Pb isotopic variation along the Pacific-Antarctic rise crest, 53-57S: Implications for the composition and dynamics of the South Pacific upper mantle: *Earth Planet. Sci. Lett.*, v. 154, p. 109-125.
- Christensen, B.P., Holm, P.M., Jambon, A., and Wilson, J.R., 2001, Helium, argon and lead isotopic composition of volcanics from Santo Antao and Fogo, Cape Verde Islands: *Chem. Geology*, v. 178, p. 127-142.

- Christie, D.M., West, B.P., Douglas, G.P., and Hanan, B.B., 1998, Chaotic topography, mantle flow and mantle migration in the Australian-Antarctic Discordance: *Nature*, v. 394, p. 637-643.
- Coffin, M.F., Pringle, M.S., Duncan, R.A., Gladchenko, T.P., Storey, M., Mueller, R.D., and Gahagan, L.A., 2002, Kerguelen hotspot magma output since 130Ma: *J. Petrology*, v. 43, p. 1121-1139.
- Dickin, A.P., 1995, *Radiogenic isotope geology*, 2nd ed., Cambridge Univ. Press.
- Dosso, L., Bougault, H., Beuzart, P., Calvez, J.Y., and Joron, J.L., 1988, The geochemical structure of the South-East Indian Ridge: *Earth Planet. Sci. Lett.*, v. 88, p. 47-59.
- Dosso, L., Bougault, H., and Joron, J.L., 1993, Geochemical morphology of the North Mid-Atlantic Ridge, 10-24N: Trace element-isotope complementarity: *Earth Planet. Sci. Lett.*, v. 120, p. 443-462.
- Doucelance, R., Escrig, S., Moreira, M., Gariépy, C., and Kurz, M.D., 2003, Pb-Sr-He isotope and trace element geochemistry of the Cape Verde Archipelago: *Geochimica et Cosmochimica Acta*, v. 67, p. 3717-3733.
- Douglas, J., Schilling, J.G., and Fontignie, D., 1999, Plume-ridge interactions of the Discovery and Shona mantle plumes with the southern Mid-Atlantic Ridge (40-55°S): *J. Geophys. Res.*, v. 104, p. 2941-2962.
- Dupre, B., and Allegre, C.J., 1983, Pb-Sr isotope variation in Indian Ocean basalts and mixing phenomena: *Nature*, v. 303, p. 142-146.
- Ebinger, C.J., and Sleep, N.H., 1998, Cenozoic magmatism throughout east Africa resulting from impact of a single plume: *Nature*, v. 395, p. 788-791.

- Fitton, J.G., Saunders, A.D., Norry, M.J., Hardarson, B.S., and Tayler, R.N., 1997, Thermal and chemical structure of the Iceland plume: *Earth Planet. Sci. Lett.*, v. 153, p. 197-208.
- Foulger, G.R., and Pearson, D.G., 2001, Is Iceland underlain by a plume in the lower mantle? Seismology and helium isotopes: *Geophys. J. Int.*, v. 145, p. F1-5.
- Frey, F.A., Nicolaysen, K., Kubit, B.K., Weis, D., and Gret, A., 2002, Flood basalt from Mont Tourmente in the central Kerguelen archipelago: the Change from transitional to alkalic basalt at ~25Ma: *J. Petrology*, v. 43, p. 1367-1387.
- Gaboret, C., Forte, A.M., and Montagner, J.P., 2003, The unique dynamics of the Pacific Hemisphere mantle and its signature on seismic anisotropy: *Earth Planet. Sci. Lett.*, v. 208, p. 219-233.
- Graham, D.W., Castillo, P.R., Lupton, J.E., and Batiza, R., 1996, Correlated He and Sr isotope ratios in South Atlantic near-ridge seamounts and implications for mantle dynamics: *Earth Planet. Sci. Lett.*, v. 144, p. 491-503.
- Graham, D.W., Jenkins, W.J., Schilling, J.G., Thompson, G., Kurz, M.D., and Humphris, S.E., 1992, Helium isotope geochemistry of mid-ocean ridge basalts from the South Atlantic: *Earth Planet. Sci. Lett.*, v. 110, p. 133-147.
- Graham, D.W., Johnson, K.T.M., Priebe, L.D., and Lupton, J.E., 1999, Hotspot-ridge interaction along the Southeast Indian Ridge near Amsterdam and St. Paul islands: helium isotope evidence: *Earth Planet. Sci. Lett.*, v. 167, p. 297-310.
- Graham, D.W., Lupton, J.E., Spera, F.J., and Christie, D.M., 2001, Upper-mantle dynamics revealed by helium isotope variations along the Southeast Indian Ridge: *Nature*, v. 409, p. 701-703.

- Gurnis, M., Louis, M., and Mueller, R.D., 2000, Models of mantle convection incorporating plate tectonics: the Australian region since the Cretaceous, *in* M.A. Richards, R.G.G.a.R.D.v.d.H., ed., The history and dynamics of global plate motions, Volume 121: Washington, DC., Geophys. Monogr. Ser. AGU, p. 211-238.
- Hanan, B.B., Kingsley, R.H., and Schilling, J.G., 1986, Pb isotope evidence in the South Atlantic for migrating ridge-hotspot interactions: *Nature*, v. 322, p. 137-144.
- Hart, S.R., 1984, A large-scale isotope anomaly in the Southern Hemisphere mantle: *Nature*, v. 309, p. 753-757.
- Hilton D. R., Thirlwall, M.F., Tayler, R.N., Murton, B.J., and Nichols, A., 2000, Controls on magmatic degassing along the Reykjanes Ridge with implications for the helium paradox: *Earth Planet. Sci. Lett.*, v. 183, p. 43-50.
- Hilton, D.R., Barling, J., and Wheller, G.E., 1995, Effect of shallow-level contamination on the helium isotope systematics of ocean-island lavas: *Nature*, v. 373, p. 330-333.
- Johnson, K., Graham, D.W., Rubin, K., Nicolaysen, K., Scheirer, D., Forsyth, D., Baker, E., and Douglas-Priebe, L., 2000, Boomerang Seamount: the active expression of the Amsterdam-St.Paul hotspot, Southeast Indian Ridge: *Earth Planet. Sci. Lett.*, v. 183, p. 245-259.
- Kido, M., and Seno, T., 1994, Dynamic topography compared with residual depth anomalies in oceans and implications for age-depth curves: *Geophys. Res. Lett.*, v. 21, p. 717-720.

- Larson, R.L., 1991, Geological consequences of super plumes: *Geology*, v. 19, p. 963-966.
- Lehnert, K., Su, Y., Langmuir, C.H., Sarbas, B., and Nohl, U., 2000, A global geochemical database structure for rocks: *Geochem. Geophys. Geosyst.*, v. 1, p. 1999GC000026.
- Leveque, J.J., Debayle, E., and Maupin, V., 1998, Anisotropy in the Indian Ocean upper mantle from Rayleigh- and Love-waveform inversion: *Geophys. J. Int.*, v. 133, p. 529-540.
- Macdougall, J.D., and Lugmair, G.W., 1986, Sr and Nd isotopes in basalts from the East Pacific Rise: significance for mantle heterogeneity: *Earth Planet. Sci. Lett.*, v. 77, p. 273-284.
- Mahoney, J., LeRoex, A.P., Peng, A., Fisher, R.L., and Natland, J.H., 1992, Southwestern limits of Indian Ocean Ridge mantle and the origin of low  $^{206}\text{Pb}/^{204}\text{Pb}$  mid-ocean ridge basalt: Isotope systematics of the Central Southwest Indian Ridge (17-50°E): *J. Geophys. Res.*, v. 97, p. 19771-19790.
- Mahoney, J., Natland, J.H., White, W.M., Poreda, R., Bloomer, S.H., Fisher, R.L., and Baxter, A.N., 1989, Isotopic and geochemical provinces of the Western Indian Ocean spreading centers: *J. Geophys. Res.*, v. 94, p. 4033-4052.
- Mahoney, J.J., Graham, D.W., Christie, D.M., Johnson, K.T.M., Hall, L.S., and Vonderhaar, D.L., 2002, Between a hotspot and a cold spot: Isotopic variation in the Southeast Indian Ridge athenosphere, 86E-118E: *J. Petrology*, v. 43, p. 1155-1176.

- Mahoney, J.J., Sinton, J.M., Kurz, M.D., Macdougall, J.D., Spencer, K.J., and Lugmair, G.W., 1994, Isotope and trace element characteristics of a super-fast spreading ridge: East Pacific rise, 13-23°S: *Earth Planet. Sci. Lett.*, v. 121, p. 173-193.
- Marks, K.M., and Stock, J.M., 1994, Variation in ridge morphology and depth-age relationships on the Pacific-Antarctic ridge: *J. Geophys. Res.*, v. 99, p. 531-541.
- McNutt, M.K., and Fischer, K.M., 1987, The South Pacific Superswell, *in* Keating, B.H., Fryer, P., Batiza, R., and Boehlert, G.W., eds., *Seamounts, Islands, and Atolls*, Volume Geophysical Monograph #43, American Geophysical Union, p. 25-34.
- Meibom, A., Anderson, D.L., Sleep, N.H., Frei, R., Chamberlain, C.P., Hren, M.T., and Wooden, J.L., 2003, Are high  $^3\text{He}/^4\text{He}$  ratios in oceanic basalts an indicator of deep-mantle plume components?: *Earth Planet. Sci. Lett.*, v. 208, p. 197-204.
- Michard, A., Montigny, R., and Schlich, R., 1986, Geochemistry of the mantle beneath the Rodriguez Triple Junction and the South-East Indian Ridge: *Earth Planet. Sci. Lett.*, v. 78, p. 104-114.
- Montagner, J.P., and Guillot, L., 2002, Seismic anisotropy and global geodynamics: Plastic deformation of minerals and rocks, *Rev. Mineral. Geochem.*, Volume 51: Washington, D.C. , Mineral. Soc. Am., p. 353-385.
- Montagner, J.P., and Tanimoto, T., 1990, Global anisotropy in the upper mantle inferred from the regionalization of phase velocities: *J. Geophys. Res.*, v. 95, p. 4797-4819.
- Morgan, W.J., 1978, Rodriguez, Darwin, Amsterdam....., A second type of hotspot island: *J. Geophys. Res.*, v. 83, p. 5355-5360.

- Morgan, W.J., and Phipps Morgan, J., in press, Plate Velocities in the Hotspot Reference Frame, *in* Foulger, G.R., and Jurdy, D., eds., Plates, Plumes, and Planetary Processes: Geological Society of America Special Paper ###.
- Neves, M.C., Searle, R.C., and Bott, M.H., 2003, Easter microplate dynamics: *J. Geophys. Res.*, v. 108, p. doi:10.1029/2001JB000908.
- Niu, Y., Collerson, K.D., Batiza, R., Wendt, J.I., and Regelous, M., 1999, Origin of enriched type mid-ocean ridge basalt at ridges far from mantle plumes: The East Pacific Rise at 11°20'N: *J. Geophys. Res.*, v. 104, p. 7067-7087.
- Parmentier, E.M., and Oliver, J.E., 1979, A study of shallow mantle flow due to the accretion and subduction of lithospheric plates: *Geophys. J. R. Astron. Soc.*, v. 57, p. 1-22.
- Parmentier, E.M., and Sotin, C., 2000, Three-dimensional numerical experiments on thermal convection in a very viscous fluid: Implications for the dynamics of a thermal boundary layer at high Rayleigh number: *Physics of Fluids*, v. 12, p. 609-617.
- Peate, D.W., Hawkesworth, C.J., van Calsteren, P.W., Taylor, R.N., and Murton, B.J., 2001, <sup>238</sup>U-<sup>230</sup>Th constraints on mantle upwelling and plume-ridge interaction along the Reykjanes Ridge: *Earth Planet. Sci. Lett.*, v. 187, p. 259-272.
- Phipps Morgan, J., 1997, The Generation of a Compositional Lithosphere by Mid-Ocean Ridge Melting and its Effect on Subsequent Off-Axis Hotspot Upwelling and Melting: *Earth Planet. Sci. Lett.*, v. 146, p. 213-232.
- , 1999, The isotope topology of individual hotspot basalt arrays: Mixing curves or melt extraction trajectories?: *Geochemistry, Geophysics, Geosystems*, v. 1.

- Phipps Morgan, J., Hasenclever, J., Hort, M., Rüpke, L., and Parmentier, E.M., 2006, On subducting slab entrainment of buoyant asthenosphere: *Terra Nova*, v. in press.
- Phipps Morgan, J., and Morgan, W.J., 1999, Two-stage melting and the geochemical evolution of the mantle: a recipe for mantle plum-pudding: *Earth Planet. Sci. Lett.*, v. 170, p. 215-239.
- Phipps Morgan, J., Morgan, W.J., Zhang, Y.-S., and Smith, W.H.F., 1995, Observational hints for a plume-fed sub-oceanic asthenosphere and its role in mantle convection: *J. Geophys. Res.*, v. 100, p. 12753-12768.
- Phipps Morgan, J., and Smith, W.H.F., 1992, Flattening of the seafloor depth-age curve as a response to asthenospheric flow: *Nature*, v. 359, p. 524-527.
- Poreda, R., Schilling, J.-G., and Craig, H., 1986, Helium and hydrogen isotopes in ocean-ridge basalts north and south of Iceland: *Earth Planet. Sci. Lett.*, v. 78, p. 1-17.
- Price, R.C., Kennedy, A.K., Sneeringer, M.R., and Frey, F.A., 1986, Geochemistry of basalts from the Indian Ocean triple junction: implications for the generation and evolution of Indian Ocean ridge basalts: *Earth Planet. Sci. Lett.*, v. 78, p. 379-396.
- Ritsema, J., and Allen, R., 2003, The elusive mantle plume: *Earth Planet Sci. Lett.*, v. 207, p. 1-12.
- Royer, J.-Y., and Sandwell, D.T., 1989, Evolution of the Eastern Indian Ocean since the late Cretaceous: Constraints from geosat altimetry: *J. Geophys. Res.*, v. 94, p. 13755-13782.
- Rubin, K., and Mahoney, J., 1993, What's on the plume channel?: *Nature*, v. 362, p. 109-110.

- Schilling, J.-G., 1973, Iceland mantle plume: Geochemical study of Reykjanes Ridge: *Nature*, v. 242, p. 565-571.
- Schilling, J.-G., Hanan, B.B., McCully, B., and Kingsley, R.H., 1994, Influence of the Sierra Leone mantle plume on the equatorial Mid-Atlantic Ridge: A Nd-Sr-Pb isotopic study: *J. Geophys. Res.*, v. 99, p. 12005-12028.
- Schilling, J.-G., Thompson, G., Kingsley, R.H., and Humphris, S.E., 1985, Hotspot-migrating ridge interaction in the South Atlantic: *Nature*, v. 313, p. 187-191.
- Schouten, H., Klitgord, K.D., and Gallo, D.G., 1993, Edge-driven microplate kinematics: *Journal of Geophysical Research*, v. 98, p. 6689-6702.
- Sempere, J.C., Cochran, J.R., and team, S.S., 1997, The southeast Indian Ridge between 88°E and 118°E: Variations in crustal accretion at constant spreading rate: *J. Geophys. Res.*, v. 102, p. 15489-15505.
- Small, C., 1995, Observation of ridge-hotspot interactions in the Southern Ocean: *J. Geophys. Res.*, v. 100, p. 17931-17946.
- Small, C., Cochran, J.R., Sempere, J.C., and Christie, D.M., 1999, The structure and segmentation of the South Indian Ridge: *Marine Geology*, v. 161, p. 1-12.
- Sotin, C., and Labrosse, S., 1999, Three-dimensional convection in an iso-viscous, infinite Prandtl number fluid heated from within and from below: applications to the transfer of heat through planetary mantles: *Earth Planet. Sci. Lett.*, v. 112, p. 171-190.
- Staudacher, T., Sarda, P., Richardson, S.H., Allegre, C.J., Sagna, I., and Dmitriev, L.V., 1989, Noble gases in basalt glasses from a Mid-Atlantic Ridge topographic high at 14N: Geodynamic consequences: *Earth Planet. Sci. Lett.*, v. 96, p. 119-133.

- Staudigel, H., Park, K.-H., Pringle, M.S., Rubenstone, J.L., Smith, W.H.F., and Zindler, A., 1991, The longevity of the South Pacific isotopic and thermal anomaly: *Earth Planet. Sci. Lett.*, v. 102, p. 24-44.
- Taylor, R.N., Thirlwall, M.F., Murton, B.J., Hilton, D.R., and Gee, M.A.M., 1997, Isotopic constraints on the influence of the Icelandic plume: *Earth Planet. Sci. Lett.*, v. 148, p. E1-E8.
- Veevers, J.J., 1982, Australian-Antarctic depression from the mid-ocean ridge to adjacent continents: *Nature*, v. 295, p. 315-317.
- Vlastelic, I., Aslanian, D., Dosso, L., Bougault, H., Olivet, J.L., and Geli, L., 1999 Large-scale chemical and thermal division of the Pacific mantle: *Nature*, v. 399, p. 345-350.
- Vlastelic, I., Dosso, L., Bougault, H., Aslanian, D., Geli, L., Etoubleau, J., Bohn, M., Joron, J.L., and Bollinger, C., 2000, Chemical systematics of an intermediate spreading ridge: The Pacific-Antarctic Ridge between 56S and 66S: *J. Geophys. Res.*, v. 105, p. 2915-1936.
- Vogt, P.R., 1971, Asthenosphere motion recorded by the ocean floor south of Iceland: *Earth Planet. Sci. Lett.*, v. 13, p. 153-160.
- Vogt, P.R., and Johnson, L., 1972, Seismic reflection survey of an oblique aseismic basement trend on the Reykjanes Ridge: *Earth Planet. Sci. Lett.*, v. 15, p. 248-254.
- , 1975, Transform faults and longitudinal flow below the midoceanic ridge: *J. Geophys. Res.*, v. 80, p. 1399-1428.

- Weis, D., and Frey, F.A., 2002, Submarine basalts of the northern Kerguelen Plateau: Interaction between the Kerguelen plume and the Southeast Indian Ridge revealed at ODP SITE 1140: *J. Petrology*, v. 43, p. 1287-1309.
- White, R.S., 1993, Melt production rates in mantle plumes: *Phil. Trans. Roy. Soc. London A*, v. 342, p. 137-153.
- Woodward, R.L., and Masters, G., 1991, Global upper mantle structure from long-period differential travel times: *J. Geophys. Res.*, v. 96, p. 6351-6377.
- Yale, M.M., and Phipps Morgan, J., 1998, Asthenosphere flow model of hotspot-ridge interactions: a comparison of Iceland and Kerguelen: *Earth Planet. Sci. Lett.*, v. 161, p. 45-56.
- Ying, M., and Cochran, J.R., 1996, Transitions in axial morphology along the Southeast Indian Ridge: *J. Geophys. Res.*, v. 101, p. 15849-15866.
- Zindler, A., and Hart, S., 1986, Chemical Geodynamics: *Annual Review of Earth and Planetary Sciences*, v. 14, p. 493-571.

## FIGURE CAPTIONS

### *Figure 1*

Global asthenosphere flow model. Arrows represent total flux (=pressure-induced flow + shear-induced flow) and color shows the lateral pressure field associated with this flow expressed as dynamic topography. This preferred solution for the predicted largescale pattern of global asthenospheric flow is based upon the absolute plate motions shown in Table 1 and relative plume strengths shown in Table 2 of the companion paper [“Global Plume-fed Asthenosphere Flow: (1) Motivation and Model Development”, this volume.]. The companion paper contains a detailed description of the modeling approach and model assumptions.

### *Figure 2*

Plume provinces in the North Atlantic and plume influences along the northern Mid-Atlantic Ridge.

a) Plume provinces in North Atlantic. Different colors show different plume sources calculated by forward-tracking from the source plumes, under the assumption that the calculated present-day flow pattern represents steady-state asthenosphere flow. Only one color may be visible in an area where actually several plume materials run though because colors can overprint other colors.

b) Plume influence along the ridge. This plot shows which regions along the ridge are fed from which plumes. The same color-coding is used for plumes as in Figure 2a. Triangles show the source plume's latitude (or longitude, depending on the axis-scale in the figure panel).

*Figure 3*

Plume provinces in the South Atlantic and plume influences along the southern Mid-Atlantic Ridge.

See caption to Figure 2 for description of plotting conventions.

*Figure 4*

Plume provinces in the southern Indian Ocean and plume influences along the South West Indian Ridge (SWIR).

See caption to Figure 2a for description of plotting conventions.

Note that asthenosphere in this region is fed from many different plume sources including those in the south Atlantic that cross the spreading center near the Rodrigues Triple Junction (RTJ).

*Figure 5*

Plume provinces in the southern Indian Ocean and plume influences along the South East Indian Ridge (SEIR). See caption to Figure 2 for description of plotting conventions.

*Figure 6*

Plume provinces in the Pacific Ocean and plume influences along the East Pacific Rise (EPR). See caption to Figure 2 for description of plotting conventions. Note that the fastest spreading ridge on EPR around 30°S ‘pulls’ a large amount of plume materials from beneath the Pacific Plate. Note, too, the ‘vortex’ pattern of asthenosphere flow beneath this region.

*Figure 7*

Along-axis bathymetric [Vogt, 1986] and geochemical [Dosso *et al.*, 1993] variations along the northern Mid-Atlantic Ridge (figure from Phipps Morgan *et al.* [1995]). All geochemical “spikes” along the ridge seem to be associated with ridge segments that are closest to a neighboring hotspot. Phipps Morgan *et al.* [1995] suggested the interaction of each spike and the hotspot in the same latitude. This study supports their interpretation for regions surrounding Iceland and the Azores, however, it does not support their suggestion for a flow-connection between the Cape Verde plume and the 14°N spike.

*Figure 8*

Axial variation of  $^4\text{He}/^3\text{He}$ ,  $^{206}\text{Pb}/^{204}\text{Pb}$ ,  $^{208}\text{Pb}/^{204}\text{Pb}$  and (La/Sm) along the southern MAR [Graham *et al.* 1992]. Geochemical spikes occur at the same latitude along the ridge as that of nearby hotspots and show no variation – except in  $^4\text{He}/^3\text{He}$  -- along the ridge in the region between 20°S and 30°S where there are no off-axis hotspots. See discussion in text.

*Figure 9*

Longitudinal patterns of  $^{206}\text{Pb}/^{204}\text{Pb}$ ,  $^{87}\text{Sr}/^{86}\text{Sr}$ ,  $(^3\text{He}/^4\text{He})/(^3\text{He}/^4\text{He})_{\text{atm}}$  and axial depth [Mahoney *et al.*, 2002] along the Southeast Indian Ridge (SEIR). The along-ridge isotopic peak appears eastward of St. Paul hotspot, suggesting that St. Paul is not the source for eastward-flowing asthenospheric flow along the SEIR. Note that the western edge of a plume's influence lies at each  $^3\text{He}/^4\text{He}$  peak. The large influence area of the Kerguelen plume is consistent with the idea that this is the strongest plume in this region and agrees with the ridge's shallow topography and axial high morphology [Ying and Cochran, 1996] in the region of Kerguelen plume influence. See discussion in text.

*Figure 10*

$\delta(\text{Sr-Pb})$  along the Pacific spreading system from [Vlastelic *et al.*, 1999] The color of the square is related to the sign of the deviation from a reference line: green indicates a positive deviation while red shows a negative deviation. The size of each

square is proportional to the absolute deviation value. The inset at top left shows  $\delta(\text{Sr-Pb})$  versus ridge depth. See discussion in text.

*Figure 11*

$^3\text{He}/^4\text{He}$ ,  $^{21}\text{Ne}/^{22}\text{Ne}$ , Sr-, Nd-, and Pb-isotopes in MORB as a function of their latitude along the EPR [Mahoney *et al.*, 1994]. Isotope values are displayed as a fraction of their minimum to maximum isotopic values along this section of the global ridge system. Color bars show plume influences along the ridge. See discussion in text.

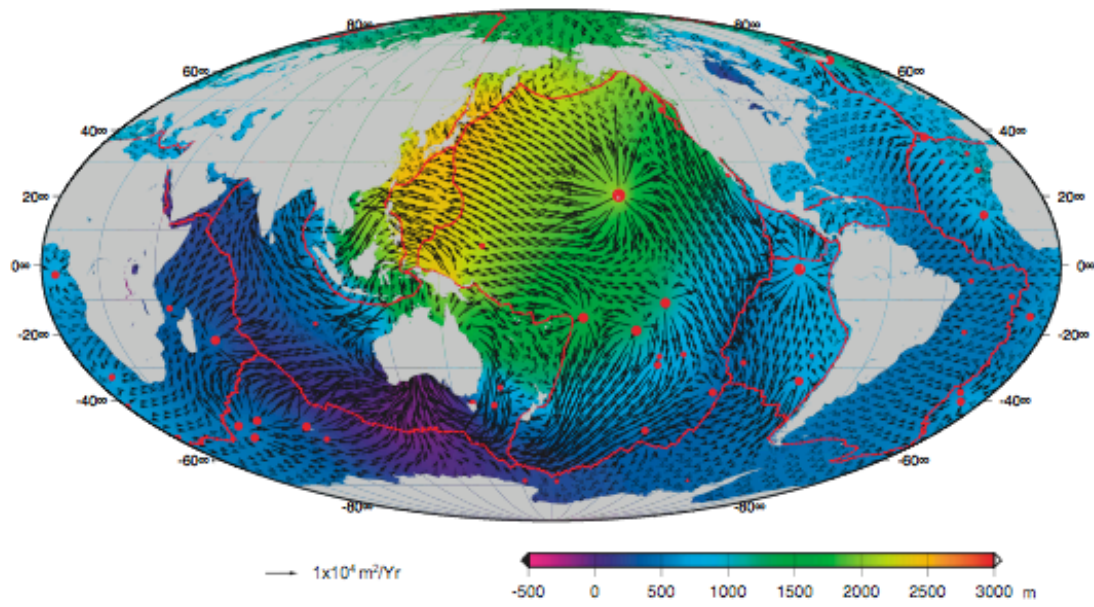


Figure 1

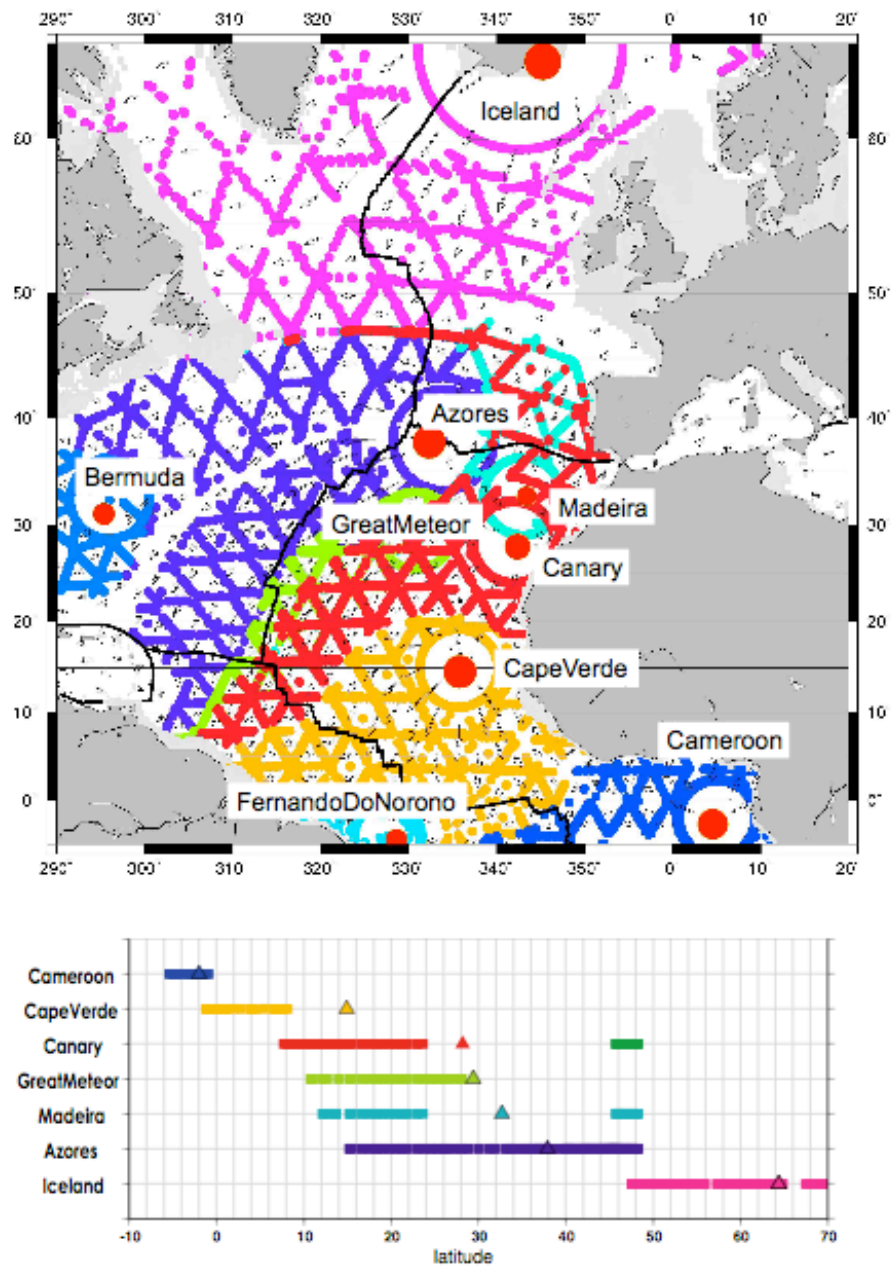


Figure 2

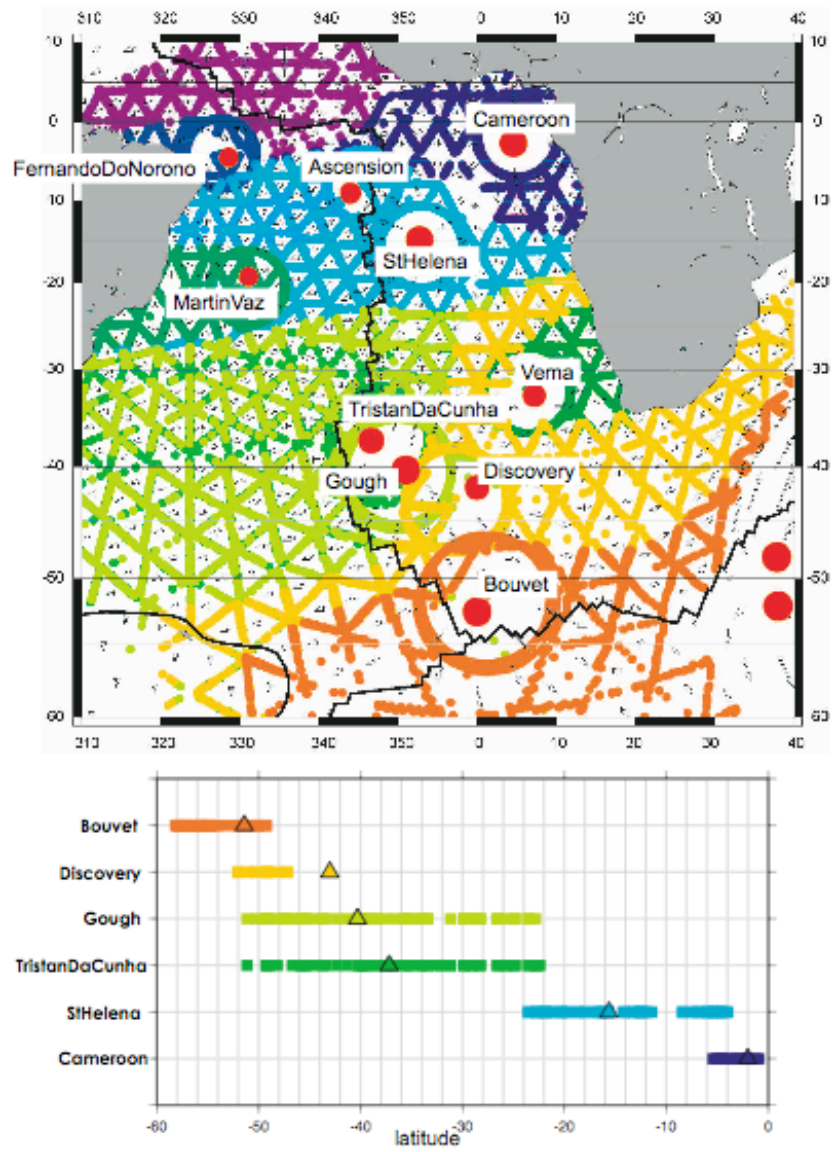


Figure 3

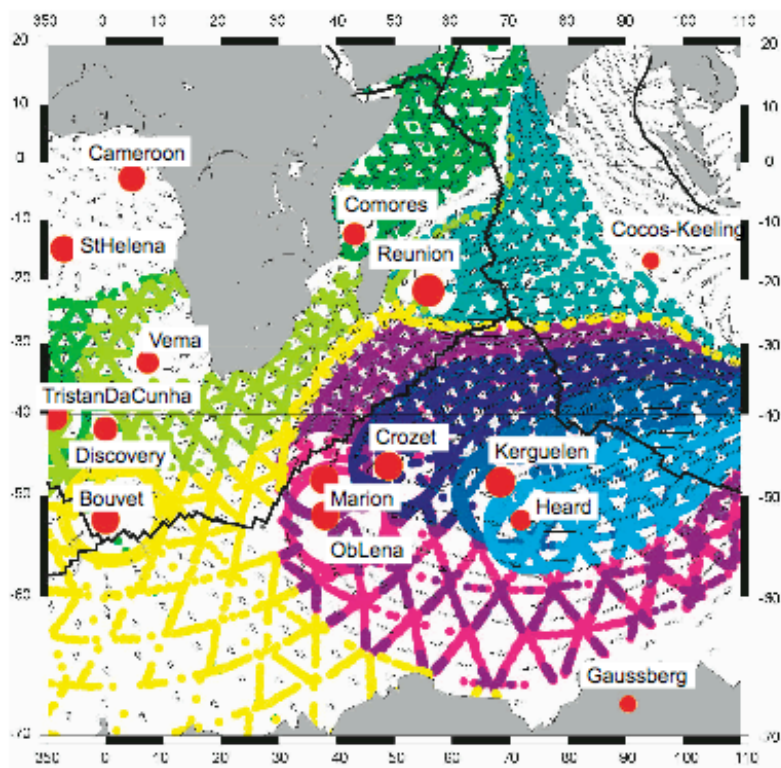


Figure 4

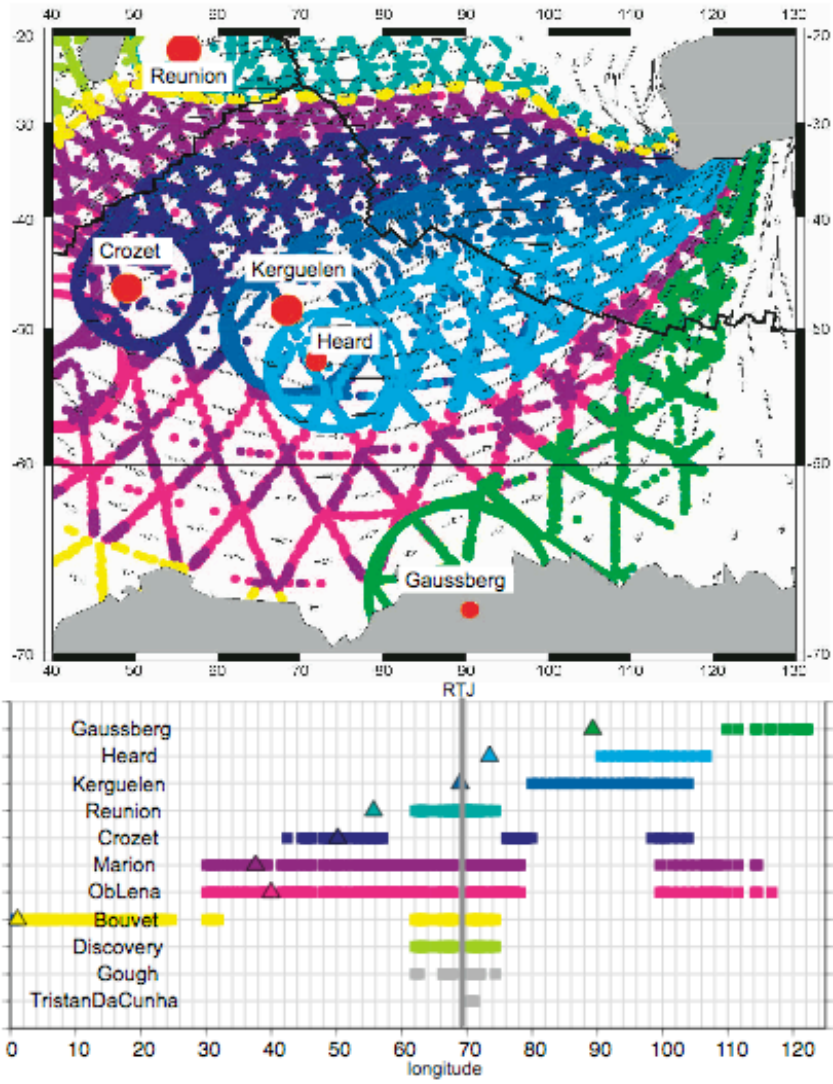


Figure 5

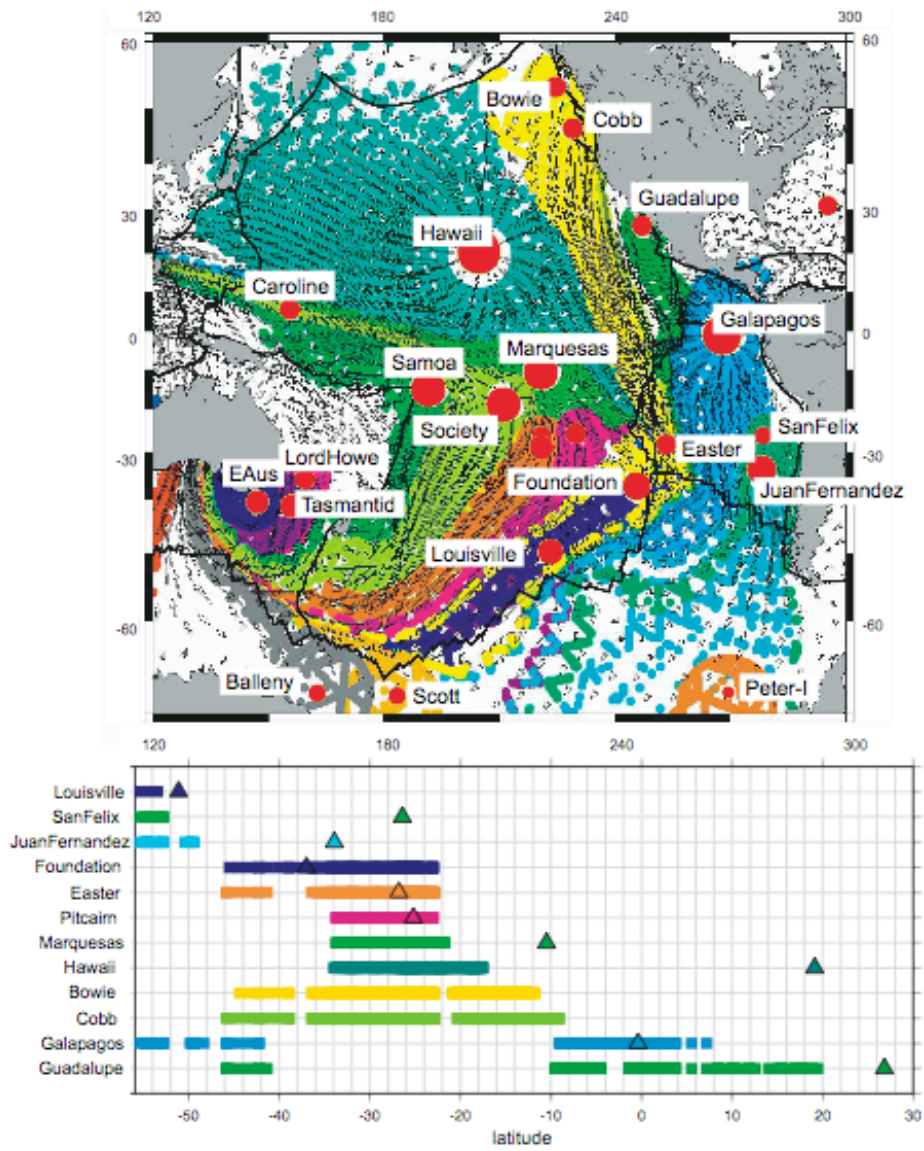
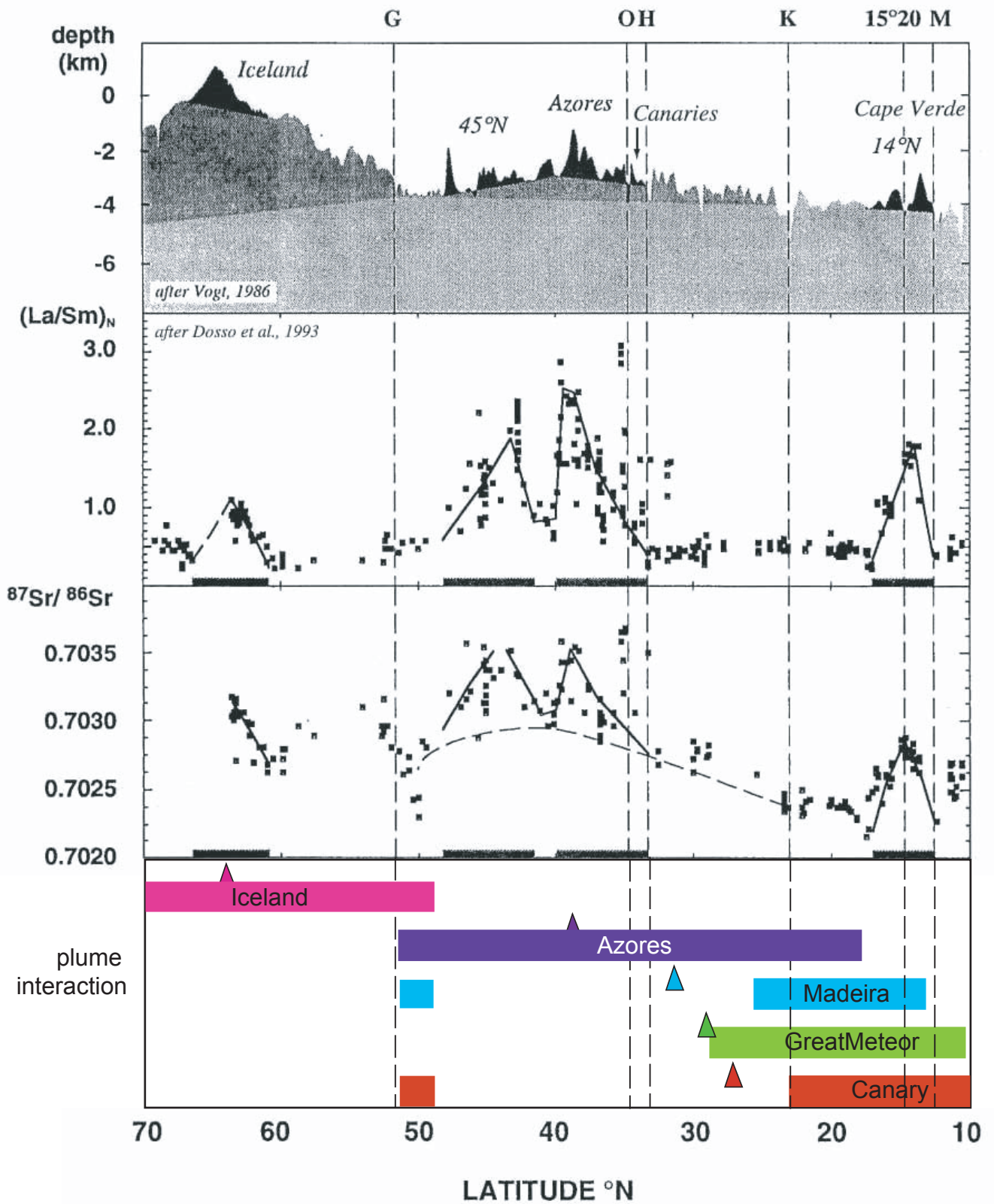
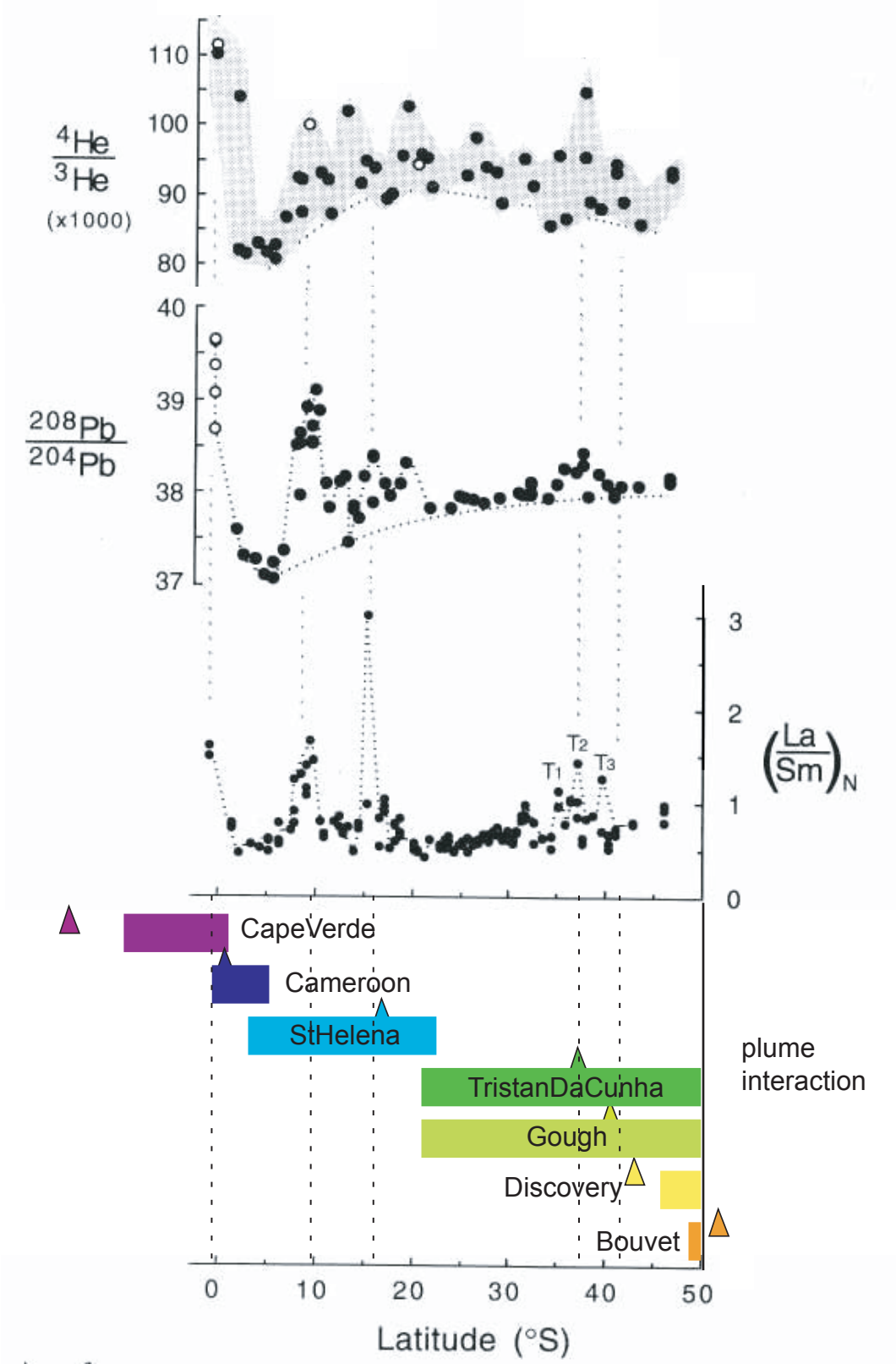
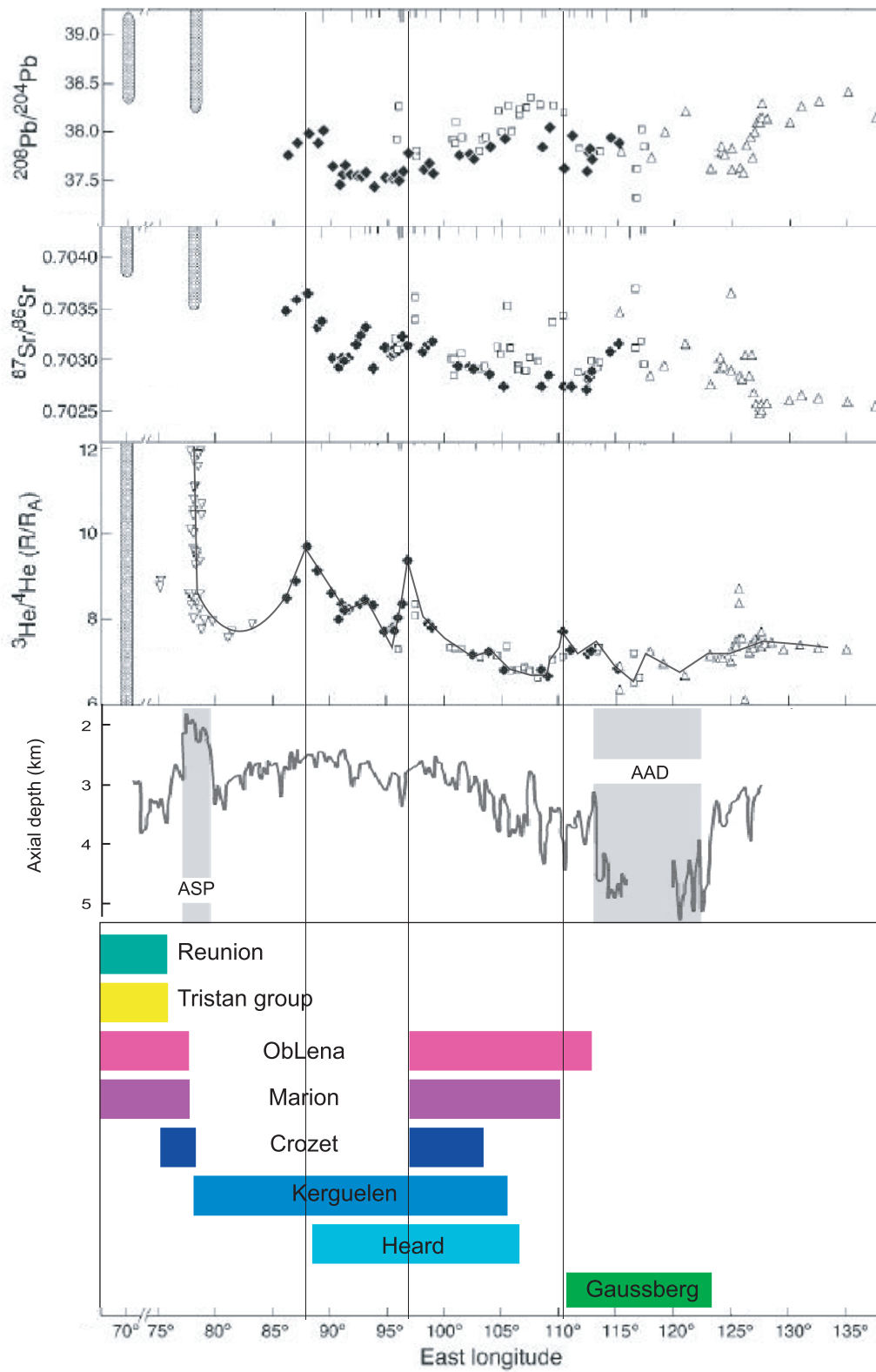


Figure 6







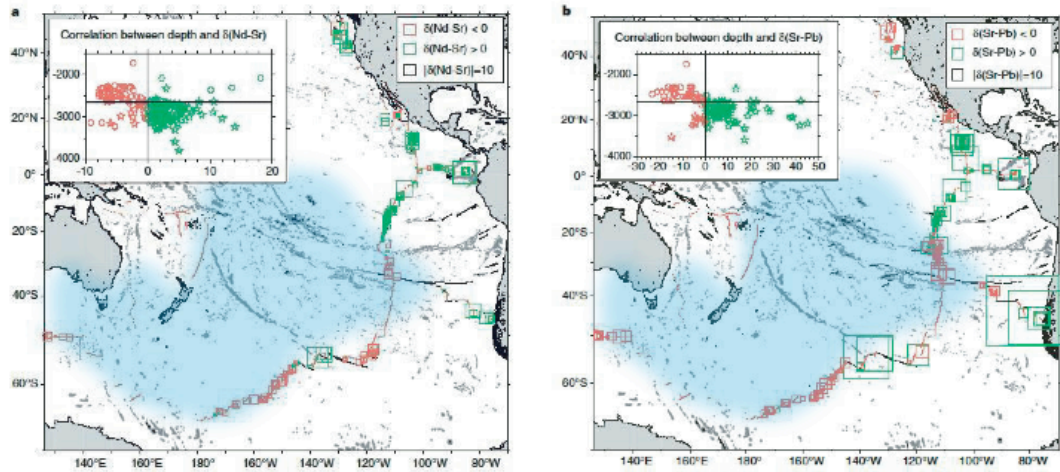


Figure 10

